Endospore Appendages

Subjects: Cell Biology

Contributor: Ephrem Zegeye

The endospores (spores) of many *Bacillus cereus* sensu lato species are decorated with multiple hair/pilus-like appendages. Although they have been observed for more than 50 years, all efforts to characterize these fibers in detail have failed until now, largely due to their extraordinary resilience to proteolytic digestion and chemical solubilization. A recent structural analysis of *B. cereus* endospore appendages (Enas) using cryo-electron microscopy has revealed the structure of two distinct fiber morphologies: the longer and more abundant "Staggered-type" (S-Ena) and the shorter "Ladder-like" type (L-Ena), which further enabled the identification of the genes encoding the S-Ena. Ena homologs are widely and uniquely distributed among *B. cereus* sensu lato species, suggesting that appendages play important functional roles in these species. The discovery of *ena* genes is expected to facilitate functional studies involving Ena-depleted mutant spores to explore the role of Enas in the interaction between spores and their environment.

endospore spore appendage Bacillus cereus Ena

1. Endospore Appendages

The existence of hair/pilus-like endospore appendages (hereafter called Enas) on spore surfaces was reported already in the 1960s [1][2]. Ankolekar *et al*. showed that all 47 tested food isolates of *B. cereus* are endowed with Enas. Enas were also found in ten of 12 enterotoxigenic food isolates of *B. thuringiensis* [3]. Whereas the presence of Enas appears to be a general characteristic of *B. cereus* sensu stricto (s.s.) and *B. thuringiensis* spores, they have not been observed on *B. anthracis* or *B. sphaericus* spores [3][4][5], nor on spores of any species belonging to the *B. subtilis* group [5]. Variations in the number of Enas per spore and their morphology have been observed even between strains of the same species. For example, among seven strains of *B. cereus* examined, the number of Enas per spore ranged from one to 23, with an average of five to eight Enas [6], and length ranged from 0.6 to 2 µm [6]. Another strain of *B. cereus* displayed 20–30 Enas per spore, with lengths ranging from 200 nm to 6 µm [7]. Apart from the variation in the length and number of Enas per spore, atomic force microscopy (AFM) of *B. cereus* endospores revealed a thicker type of Enas (ø 8–12 nm, length 0.4–1.2 µm) present together with a thinner type Enas (ø 2.5–3.5 nm, length 0.2–1.6 µm) [8]. Consistent with that, a recent detailed analysis of Enas from the *B. cereus* food poisoning outbreak strain NVH0075-95 using cryo-EM revealed proteinaceous Ena fibers of two distinct morphologies, named staggered (S)- and ladder (L)- Enas [8][7] (**Figure 1**A). S-Ena is the predominant form of Ena (~90%) in *B. cereus* NVH 0075-95 [7], which presumably corresponds to the thicker type of Ena reported earlier [8]. Interestingly, while the S-Ena appears to be connected to the endospore coat and traverses the exosporium, the L-Ena emerges from the exosporium [8][7].

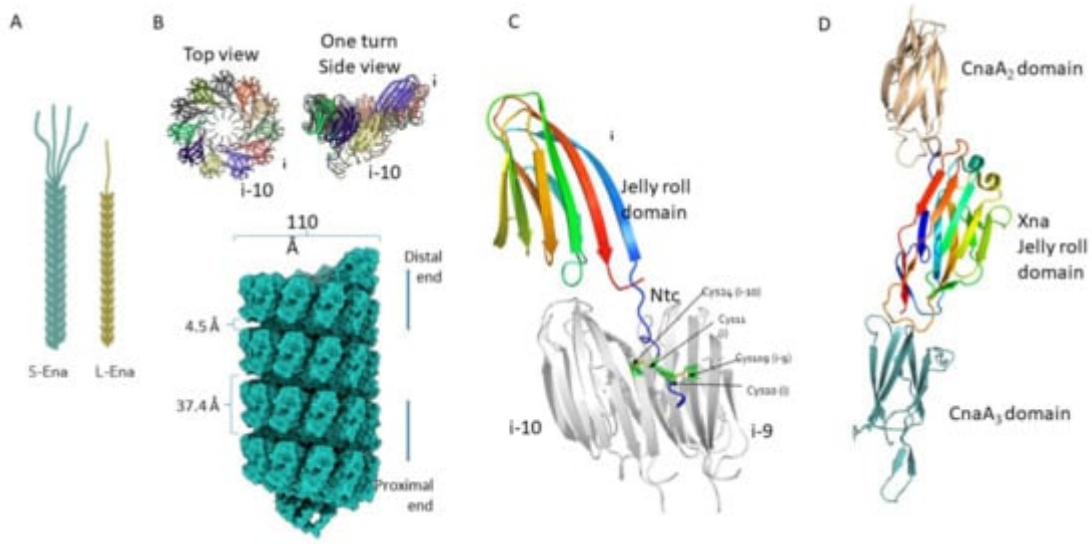

Figure 1. The architecture of the Ena fibers. (A) Illustration of S-Ena and L-Ena fibers with staggered and ladder-like arrangements of Ena subunits, respectively. In their termini distal to the endospore, the S-Ena fiber has ~4–5 ruffles (thin filamentous extensions of ~4 nm diameter), while the L-Ena has a single ruffle. (**B**) Surface representation of the atomic model of four helical turns of the S-Ena. Side and top view of one S-Ena helical turn featuring a ribbon representation of β–strands. (**C**) Three connected Ena subunits (as viewed from the central axis of the fiber or exposing the interior) highlighting the jelly roll domain and the *N*-terminal connector (Ntc) (PDB ID 7A02). Arrows point to Cys10, Cys11 of the Ntc from ith subunit that is involved in the disulphide linkage with Cys109, Cys24 of the i-9th and the i-10th subunits, respectively. Reprinted from [7].(**D**) Example of Gram-positive pilin with its Cna domains. Shown here is BcpA, the major pilin of *B. cereus* vegetative pili (PDB ID 3KPT), highlighting the $CnaA_2$, $CnaA_3$, and Xna domains in light orange, light cyan, and rainbow, respectively [9]. The CnaA domains are composed of two juxtaposed β-sheets of 3–4 strands each, while the Xna domain with a jelly roll topology consists of β-sheets of four to five strands each.

Although pili have been well-studied structurally and functionally in both Gram-negative and Gram-positive bacteria, spore appendages as a distinct class of pili are just beginning to be characterized. Some of the well-known classes of pili are chaperone-usher pili, type V pili, type IV pili, curli, fap fibers, conjugative, type IV secretion pili, e-pili in Gram-negatives, and sortase-mediated pili, and type IV pili in Gram-positive bacteria [10]. Among Gram-positives, Enas are the third class of pili to be structurally characterized [7]. Until recently, the only endospore appendages whose composition and genetic identity have been characterized were those of *Clostridium taeniosporum* [11]. *C. taeniosporum* has twelve ribbon-like appendages emanating from one pole of the spore. Four proteins, including a glycoprotein, constitute the appendages of *C. taeniosporum* [11]. Notably, no equivalents of these proteins/genes are present among *B. cereus* s.l. spp.

Interestingly, Enas are inherently resistant to boiling (100 °C), autoclavation, desiccation, treatment with strong reducing agents (200 mM β-mercaptoethanol), acids (1 M HCl), chaotropes (8 M urea or 6 M guanidinium chloride) and proteases (proteinase K), which hamper mass spectrometry approaches to deduce their amino acid

sequences [7][12]. Despite their sturdy nature [7], Ena fibers can be dislodged from the endospore body by sonication [13] or by treatment with sodium thioglycolate [14].

2. Architecture of Ena Fibers

The advent of cryo-electron microscopy (cryo-EM) has enabled us to image biological macromolecules down to the atomic level in their native form [15]. It can be used to determine the structure of multiprotein complexes and filaments with known or unknown genetic identities. In our recent work, we used cryo-EM to determine the electron potential map of ex-vivo purified S-Ena appendages at a resolution of 3.2 Å. At this resolution, we could clearly identify amino acids with bulky side chains that led us to recognize a hexapeptide sequence 'FCMTIRY' located in the *C*-terminal of an Ena subunit. Searching for this hexapeptide in the *B. cereus* NVH 0075-95 genome revealed the presence of *ena* genes [7]. Ex-vivo purified S-Ena is composed of Ena1A and Ena1B subunits assembled into a helix of 110 Å diameter and 37.4 Å pitch (**Figure 2**B). Each helical turn is made up of 11.6 Ena1A/B subunits (**Figure 1**B). Due to their high sequence similarity (identity, 38%; similarity, 58%) and structure, cryo-EM does not help much in unambiguously determining the stoichiometry and arrangement of EnaA/B subunits along the length of the appendages. The Ena1A/B subunits consist of a typical jelly roll fold and a 15-residue long *N*-terminal connecter (Ntc) (**Figure 1**C). A jelly roll fold generally consists of 8 β-strands arranged in two 4 stranded β-sheets juxtaposed to each other, resembling a jelly or Swiss roll cake [16]. The jelly roll domains of adjacent Ena1A/B subunits are connected to each other through β-sheet augmentation, which helps in the lateral stabilization of the helix (**Figure 1**B). Apart from that, two complementary electrostatic patches on the surfaces enhance inter-subunit contacts. The Ntc of each subunit is connected to two other subunits present in the preceding helical turn to confer longitudinal stability to the helix. Cys10 and Cys11 in the Ntc of each subunit i form disulphide bonds with Cys109 and Cys24 of subunits i-9 and i-10, respectively. The combination of β-sheet augmentation and covalent linkage through Ntc leads to the assembly of an appendage that is extremely stable, both chemically and physically [7]. Since the Ntcs are present in the luminal side of the helix, they are protected from various environmental assaults. The Ntcs are connected to the jelly roll domain through a flexible five-residue long region that creates a longitudinal gap of 4.5 Å (**Figure 1**B) between the two helical turns. Due to the flexibility of this spacer region and the lack of direct protein-protein contact between the two subunits present across different helical turns, the appendages turn out to be highly flexible. At the distal termini of the spore, both S-Ena and L-Ena have short extensions that are dubbed 'ruffles' (**Figure 1**A). The S-Ena tends to have four to five ruffles, while the L-Ena has one ruffle per appendage. When observed by negative stain TEM, the ruffles appear morphologically similar to collagen-like immunogenic hairy naps (BclA) that are found attached to the exosporium [17]; however, the protein(s) that constitute the ruffles have not yet been identified.

The jelly roll domain of Ena with its juxtaposed β-sheet architecture has previously been found in many sortase-mediated vegetative pili, such as the XNA domain in BcpA, the major subunit of the vegetative pili of *B. cereus* (**Figure 1**D) [9]. In addition to that, CnaA and CnaB-type domains found in BcpA (**Figure 1**D), SpaA pilin from *Corynebacterium diphtheriae* [18], RrgC from *Streptococcus pneumoniae* [19], and FimA and FimP from *Actonomyces oris* [20][21] are another class of domains that contain a sandwiched β-sheet architecture. Cna-

type domains are IG-like domains that consist of two juxtaposed sheets. The two sheets can be composed of either 4-4 or 4-5 β-strands (in CnaA) or 4-3 β-strands (in CnaB). These domains were first reported in *Staphylococcus aureus* as collagen-binding proteins [22]. Furthermore, triple jelly roll domains found in the C381 turret protein of *Sulfolobus* turreted icosahedral virus (STIV) are known to be involved in the interaction with the host pilus [23]. All this evidence indicates that the jelly roll domain in Enas might also play a role in adherence to host tissue.

At the domain level, Enas are similar to sortase-mediated pili of vegetative cells of other Gram-positive species. However, the arrangement of these domains in the filament is what distinguishes the two types of pili. Sortase-mediated pili consist of a linear chain of CnaA and/or CnaB domains with distinct genes for basal pilin, backbone pilin, and tip pilin and employ specific sortases to catalyze polymerization and anchoring to the peptidoglycan layer. The sortase-mediated pili rely on internal isopeptide bonds between the side chains of Lys and Asn for thermodynamic and physical stability [24][25]. On the contrary, Ena subunits assemble into a helix and undergo covalent disulphide linkages hidden inside the luminal side to survive extreme physical and chemical stress. Furthermore, Ena1A and Ena1B can self-assemble into filaments nearly identical to S-Ena in vitro [7] without the need for any specific enzyme.

3. Ena-Encoding Genes

De novo assignment of an amino acid sequence motif in the electron density map from the atomic model of the S-Ena fibers allowed identification of the protein subunits that build the Enas and the "*ena1*" genes encoding them. The *ena1* genes are located in a gene cluster consisting of *ena1A, ena1B,* and *ena1C*, encoding proteins with theoretical molecular weights of 12, 14 and 17 kDa, dubbed Ena1A, Ena1B, and Ena1C, respectively (**Figure 2**B). Knocking out any of these three genes produced spores lacking S-Ena, suggesting that all the three protein components are needed for the formation of S-Ena fibers on the surface of the spore [7]. On the other hand, the expression of the L-Ena was not affected by the absence of *ena1* genes, suggesting that the L-Ena fiber is encoded by another currently unknown gene or gene cluster located elsewhere in the bacterial genome [7]. The expression of *ena1A-C* genes was found to be concomitant with endospore formation [7].

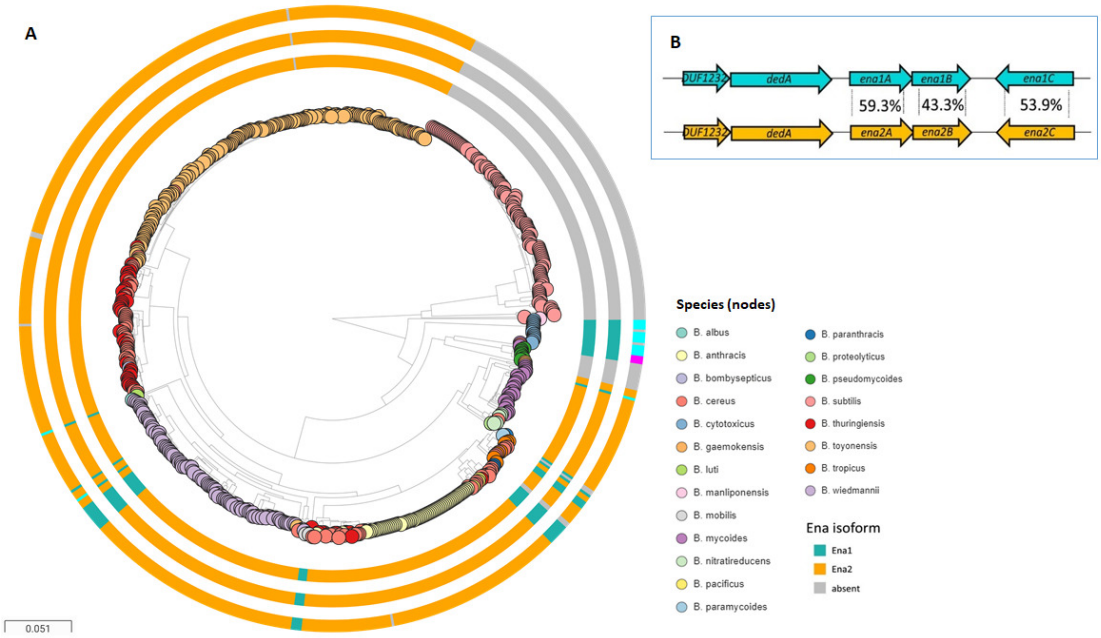

Figure 2. The *ena1* and *ena2* gene loci and distribution of these among 735 *Bacillus* genomes. (**A**) Distribution of *ena1/2A-C* among *B. cereus* s.l. spp. and the presence of genes encoding Ena subunits are indicated on surrounding rings in the following order from inner to outer: presence of *enaA*, *enaB*, and *enaC*, respectively (for all three, *ena1*: teal, *ena2*: orange, different locus: cyan). When no homolog or ortholog was found, the ring is gray. Whole genome clustering of the *B. cereus* s.l. group and *B. subtilis* created by Mashtree [26][27] and visualized in Microreact [28]. Rooted on *B. subtilis*. (**B**) (Inset) Ena1 and Ena2 loci with average amino acid sequence identity indicated between the population of EnaA-C orthologs and homologs found within the *B. cereus* s.l. group. Reprinted from [7].

4. Potential Functions of Enas

Although Enas have been known for several decades, their biological function has not yet been unraveled. In cells of Gram-negative, Gram-positive and Archaeal species, pili are involved in a multitude of functions such as adhesion to biotic and abiotic surfaces, exchange of genetic material (conjugation), natural competence, locomotion (twitching motility), biofilm formation, exoprotein secretions, electron transfer (Geobacter) and susceptibility to bacteriophages [29][30][31][32]. Pili are often involved in bacterial adhesion to a diverse range of abiotic and biotic surfaces, such as cells and tissues of plants, animals, or humans. In pathogenic species, pili have repeatedly been shown to contribute to virulence by mediating binding to mucosal surfaces [33]. Although the tip pilins found in sortase-mediated pili, for example SpaC of *Corynebacterium diphtheriae* [34], RrgA of *Streptococcus pneumoniae* [35], FimQ of *Actinomyces oris* [36], etc. are involved in cell-to-cell interaction, it remains to be determined whether Ena ruffles have analogous functions, such as in the interaction of the spores with host

receptors. Since pathogenic *Bacillus* s.l. spp. are readily transmitted to their host in the spore form [29], the Enas could play a role in the infection process by, for instance, facilitating the binding of spores to the epithelial cells of the small intestine. Indeed, the presence of ruffles at the distal ends of both S-Ena and L-Ena suggests some roles for Enas in the adhesion and/or recognition of host cell receptors or abiotic surfaces. Enas are, however, not likely to be involved in active motility or uptake/transport of DNA or proteins, as these are energy demanding processes that are not likely to occur in the endospores' metabolically dormant state. The potential roles that Enas can play in the various ecological niches of *Bacillus* spp. are summarized in **Figure 3**.

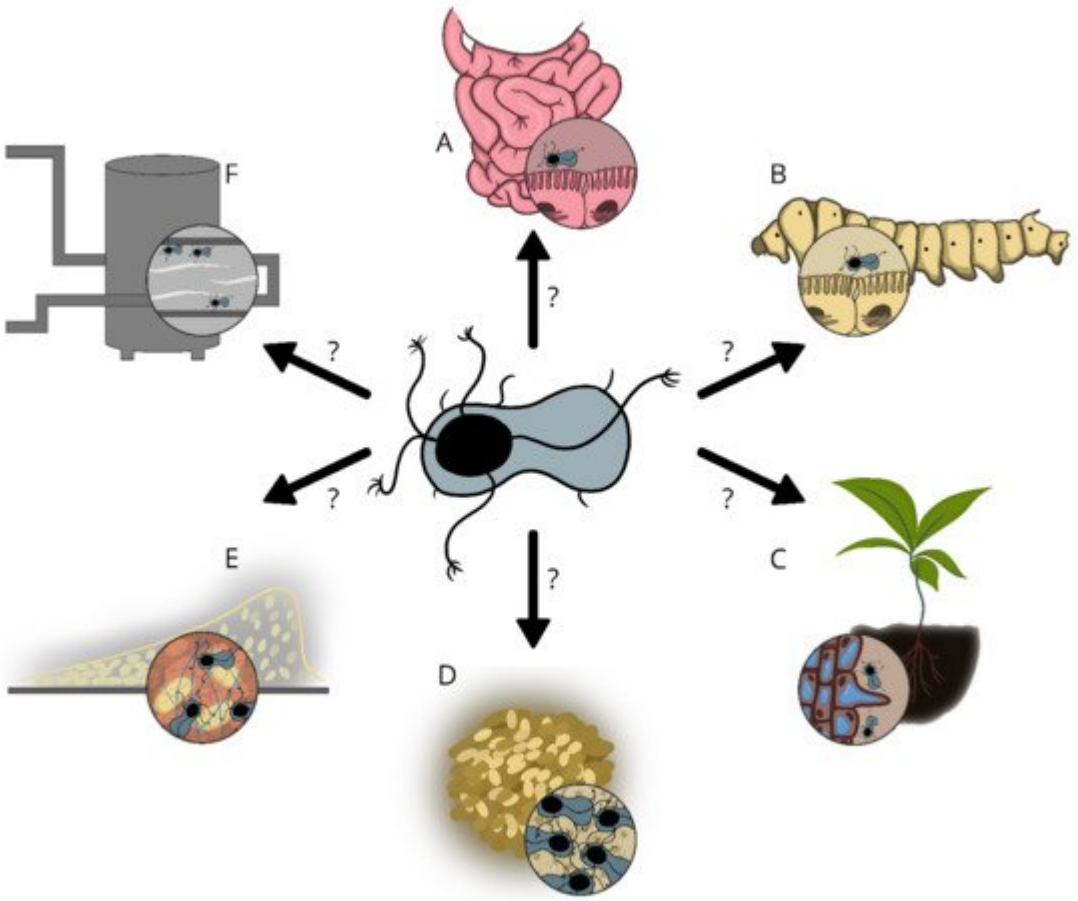

Figure 3. An illustration depicting potential roles that Enas may play in *Bacillus* s.l. spp. Adhesion of endospores to intestinal epithelial cells (**A**), insect tissues (larvae) (**B**), and plant roots (**C**). (**D**) Autoaggregation of endospores. (**E**) Biofilm formation. (**F**) Adhesion of endospores to abiotic surfaces, such as food processing surfaces. The pictures are not drawn to scale.

5. Concluding Remarks

The Enas are suggested to play a role in adhesion to biotic and/or abiotic surfaces, but sufficient experimental data are lacking. The recent discovery of the genes encoding the predominant type of Enas (S-Ena) in *B. cereus* s.l. spp.[7], is expected to facilitate comparative studies involving Ena depleted mutant spores and wild type spores. Such studies will give important insights into the function of these extraordinary fibers in spore adherence to biotic

and abiotic surfaces, biofilm formation, spore aggregation, germination, virulence, and other phenomena that would have important implications in the biology of these species. Importantly, knowledge of the potential function of Enas in spore adhesion would also allow the design of more effective strategies to prevent spore binding when harmful or promote binding when beneficial.

References

1. Rode, L.J.; Crawford, M.A.; Williams, M.G. Clostridium spores with ribbon-like appendages. J. Bacteriol. 1967, 93, 1160–1173.
2. Hachisuka, Y.; Kuno, T. Filamentous appendages of Bacillus cereus spores. Jpn. J. Microbiol. 1976, 20, 555–558.
3. Ankolekar, C.; Labbé, R.G. Physical characteristics of spores of food-associated isolates of the Bacillus cereus group. Appl. Environ. Microbiol. 2010, 76, 982–984.
4. Hachisuka, Y.; Kozuka, S. A new test of differentiation of Bacillus cereus and Bacillus anthracis based on the existence of spore appendages. Microbiol. Immunol. 1981, 25, 1201–1207.
5. Hachisuka, Y.; Kozuka, S.; Tsujikawa, M. Exosporia and appendages of spores of Bacillus species. Microbiol. Immunol. 1984, 28, 619–624.
6. Tauveron, G.; Slomianny, C.; Henry, C.; Faille, C. Variability among Bacillus cereus strains in spore surface properties and influence on their ability to contaminate food surface equipment. Int. J. Food Microbiol. 2006, 110, 254–262.
7. Pradhan, B.; Liedtke, J.; Sleutel, M.; Lindbäck, T.; Zegeye, E.D.; O'Sullivan, K.; Llarena, A.; Brynildsrud, O.; Aspholm, M.; Remaut, H. Endospore Appendages: A novel pilus superfamily from the endospores of pathogenic Bacilli. EMBO J. 2021, 40, e106887.
8. Plomp, M.; Leighton, T.J.; Wheeler, K.E.; Malkin, A.J. Architecture and high-resolution structure of Bacillus thuringiensis and Bacillus cereus spore coat surfaces. Langmuir 2005, 21, 7892–7898.
9. Budzik, J.M.; Poor, C.B.; Faull, K.F.; Whitelegge, J.P.; He, C.; Schneewind, O. Intramolecular amide bonds stabilize pili on the surface of bacilli. Proc. Natl. Acad. Sci. USA 2009, 106, 19992–19997.
10. Lukaszczyk, M.; Pradhan, B.; Remaut, H. The biosynthesis and structures of bacterial pili. In Bacterial Cell Walls and Membranes; Subcellular Biochemistry; Springer: Cham, Switzerland, 2019; Volume 92.
11. Walker, J.R.; Gnanam, A.J.; Blinkova, A.L.; Hermandson, M.J.; Karymov, M.A.; Lyubchenko, Y.L.; Graves, P.R.; Haystead, T.A.; Linse, K.D. Clostridium taeniosporum spore ribbon-like appendage structure, composition and genes. Mol. Microbiol. 2007, 63, 629–643.

12. Kozuka, S.; Tochikubo, K. Properties and origin of filamentous appendages on spores of Bacillus cereus. Microbiol. Immunol. 1985, 29, 21–37.
13. Stalheim, T.; Granum, P.E. Characterization of spore appendages from Bacillus cereus strains. J. Appl. Microbiol. 2001, 91, 839–845.
14. Kozuka, S. Fragmentation and solubilization of filamentous appendages of Bacillus cereus spores. Nippon. Saikingaku Zasshi. Jpn. J. Bacteriol. 1993, 8, 541–550.
15. Callaway, E. “It opens up a whole new universe”: Revolutionary microscopy technique sees individual atoms for first time. Nature 2020, 582, 156–157.
16. Richardson, J.S. The anatomy and taxonomy of protein structure. Adv. Protein Chem. 1981, 34, 167–339.
17. Kailas, L.; Terry, C.; Abbott, N.; Taylor, R.; Mullin, N.; Tzokov, S.B.; Todd, S.J.; Wallace, B.A.; Hobbs, J.K.; Moir, A.; et al. Surface architecture of endospores of the Bacillus cereus/anthracis/thuringiensis family at the subnanometer scale. Proc. Natl. Acad. Sci. USA 2011, 108, 16014–16019.
18. Hae, J.K.; Paterson, N.G.; Gaspar, A.H.; Hung, T.T.; Baker, E.N. The Corynebacterium diphtheriae shaft pilin SpaA is built of tandem Ig-like modules with stabilizing isopeptide and disulfide bonds. Proc. Natl. Acad. Sci. USA 2009, 106, 16967–16971.
19. Shaik, M.M.; Maccagni, A.; Tourcier, G.; Di Guilmi, A.M.; Dessen, A. Structural basis of pilus anchoring by the ancillary pilin RrgC of Streptococcus pneumoniae. J. Biol. Chem. 2014, 289, 16988–16997.
20. Mishra, A.; Devarajan, B.; Reardon, M.E.; Dwivedi, P.; Krishnan, V.; Cisar, J.O.; Das, A.; Narayana, S.V.L.; Ton-That, H. Two autonomous structural modules in the fimbrial shaft adhesin FimA mediate Actinomyces interactions with streptococci and host cells during oral biofilm development. Mol. Microbiol. 2011, 81, 1205–1220.
21. Persson, K.; Esberg, A.; Claesson, R.; Strömberg, N. The pilin protein FimP from Actinomyces oris: Crystal structure and sequence analyses. PLoS ONE 2012, 7, e48364.
22. Deivanayagam, C.C.S.; Rich, R.L.; Carson, M.; Owens, R.T.; Danthuluri, S.; Bice, T.; Höök, M.; Narayana, S.V.L. Novel fold and assembly of the repetitive B region of the Staphylococcus aureus collagen-binding surface protein. Structure 2000, 8, 67–78.
23. Hartman, R.; Eilers, B.J.; Bollschweiler, D.; Munson-McGee, J.H.; Engelhardt, H.; Young, M.J.; Lawrence, C.M. The molecular mechanism of cellular attachment for an Archaeal Virus. Structure 2019, 27, 1634–1646.
24. Khare, B.; Narayana, S.V.L. Pilus biogenesis of Gram-positive bacteria: Roles of sortases and implications for assembly. Protein Sci. 2017, 26, 1458–1473.

25. Kang, H.J.; Baker, E.N. Intramolecular isopeptide bonds give thermodynamic and proteolytic stability to the major pilin protein of Streptococcus pyogenes. J. Biol. Chem. 2009, 284, 20729–20737.
26. Katz, L.; Griswold, T.; Morrison, S.; Caravas, J.; Zhang, S.; Bakker, H.; Deng, X.; Carleton, H. Mashtree: A rapid comparison of whole genome sequence files. J. Open Source Softw. 2019, 4, 1762.
27. Ondov, B.D.; Treangen, T.J.; Melsted, P.; Mallonee, A.B.; Bergman, N.H.; Koren, S.; Phillippy, A.M. Mash: Fast genome and metagenome distance estimation using MinHash. Genome Biol. 2016, 17, 132.
28. Argimón, S.; Abudahab, K.; Goater, R.J.E.; Fedosejev, A.; Bhai, J.; Glasner, C.; Feil, E.J.; Holden, M.T.G.; Yeats, C.A.; Grundmann, H.; et al. Microreact: Visualizing and sharing data for genomic epidemiology and phylogeography. Microb. Genom. 2016, 2, e000093.
29. Swick, M.C.; Koehler, T.M.; Driks, A. Surviving between hosts: Sporulation and transmission. Microbiol. Spectr. 2016, 4, 26.
30. Petrova, O.E.; Sauer, K. Sticky situations: Key components that control bacterial surface attachment. J. Bacteriol. 2012, 194, 2413–2425.
31. Andersson, A.; Granum, P.E.; Rönner, U. The adhesion of Bacillus cereus spores to epithelial cells might be an additional virulence mechanism. Int. J. Food Microbiol. 1998, 39, 93–99.
32. Ramarao, N.; Lereclus, D. Adhesion and cytotoxicity of Bacillus cereus and Bacillus thuringiensis to epithelial cells are FlhA and PlcR dependent, respectively. Microbes Infect. 2006, 8, 1483–1491.
33. Kline, K.A.; Fälker, S.; Dahlberg, S.; Normark, S.; Henriques-Normark, B. Bacterial adhesins in host-microbe interactions. Cell Host Microbe 2009, 5, 580–592.
34. Ton-That, H.; Schneewind, O. Assembly of pili on the surface of Corynebacterium diphtheriae. Mol. Microbiol. 2003, 50, 1429–1438.
35. Izoré, T.; Contreras-Martel, C.; El Mortaji, L.; Manzano, C.; Terrasse, R.; Vernet, T.; Di Guilmi, A.M.; Dessen, A. Structural basis of host cell recognition by the pilus adhesin from Streptococcus pneumoniae. Structure 2010, 18, 106–115.
36. Wu, C.; Mishra, A.; Yang, J.; Cisar, J.O.; Das, A.; Ton-That, H. Dual function of a tip fimbrillin of Actinomyces in fimbrial assembly and receptor binding. J. Bacteriol. 2011, 193, 3197–3206.

Retrieved from https://encyclopedia.pub/entry/history/show/40141